*Neuroscience* 192 (2011) 642–651

# CHLORIDE-MEDIATED INHIBITION OF THE ICTOGENIC NEURONES INITIATING GENETICALLY-DETERMINED ABSENCE SEIZURES

**M. CHIPAUX,[a,c] S. CHARPIER[a,b*] AND P.-O. POLACK[a1]**

[a]*Centre de Recherche de l'Institut du Cerveau et de la Moelle épinière, UPMC/INSERM UMR-S 975, CNRS UMR 7225, Hôpital Pitié-Salpêtrière, F-75013, Paris, France*

[b]*UPMC Univ Paris 06, F-75005, Paris, France*

[c]*Paediatric Neurosurgery Department, Rothschild Foundation, 25 rue Manin, 75019 Paris, France*

**Abstract—Electroclinical investigations in human patients and experimental studies from genetic models demonstrated that spike-and-wave discharges (SWDs) associated with absence seizures have a cortical onset. In the Genetic Absence Epilepsy Rat from Strasbourg (GAERS), SWDs are initiated by the paroxysmal discharges of ictogenic pyramidal neurones located in the deep layers of the somatosensory cortex. However, the cellular and synaptic mechanisms that control the ictal discharges of seizure-initiating neurones remain unclear. Here, by the means of *in vivo* paired electroencephalographic (EEG) and intracellular recordings in the GAERS cortical focus, we explored the participation of the intracortical inhibitory system in the control of paroxysmal activities in ictogenic neurones. We found that their firing during EEG paroxysms was interrupted by the occurrence of hyperpolarizing synaptic events that reversed in polarity below action potential threshold. Intracellular injection of $Cl^-$ dramatically increased the amplitude of the paroxysmal depolarizations and the number of generated action potentials, strongly suggesting that the inhibitory synaptic potentials were mediated by $GABA_A$ receptors. Consistently, we showed that intracellularly recorded GABAergic interneurones fired, during seizures, shortly after (~+8 ms) the discharge of ictogenic neurones and displayed a rhythmic bursting that coincided with the inhibitory synaptic events in neighbouring pyramidal ictogenic cells. In contrast with other forms of epilepsy, our findings suggest that paroxysmal activities in the cortical pyramidal cells initiating absence seizures are negatively controlled by a feedback $Cl^-$-mediated inhibition likely resulting from the fast recurrent activation of intracortical GABAergic interneurones by the ictogenic cells themselves.** 

**Key words: absence epilepsy, inhibition, epileptic focus, cortex, interneurones, GABA.**

Absence seizures, mainly occurring in children of school age, result in transient impairments of consciousness, without convulsion, due to the abrupt appearance of spike-and-wave discharges (SWDs) over the cortical mantle and thalamic nuclei (Panayiotopoulos, 1997; Williams, 1953). Although the origin of SWDs was first attributed to functional disturbances in the intrinsic circuitry of the thalamus (Bal et al., 1995; Buzsáki, 1991), the most recent electroclinical studies in epileptic patients indicate that the onset of absence seizures is correlated with early activation of discrete cortical areas (Holmes et al., 2004; Sadleir et al., 2006; Westmijse et al., 2009). Cortical foci initiating SWDs have also been found in various rodent genetic models of absence epilepsy (Meeren et al., 2002; Polack et al., 2007, 2009). In the Genetic Absence Epilepsy Rat from Strasbourg (GAERS; Danober et al., 1998), the paroxysmal electrical activities first appear in a focus located within the facial somatosensory cortex (Polack et al., 2007). The functional inactivation of this ictogenic region prevents the occurrence of SWDs, whereas the inhibition of its related thalamic nuclei or remote cortical areas does not affect its endogenous ability to generate seizure activity (Polack et al., 2009).

Intracellular recordings in the GAERS revealed that SWDs are initiated in layer 5-6 pyramidal neurones of the cortical focus, which fire action potentials systematically before distant cortical and thalamo-cortical neurones (Polack et al., 2007, 2009). These ictogenic neurones display in between SWDs a distinctive sustained membrane depolarization and elevated tonic firing rate. This pattern of activity is converted during seizures into oscillatory-like paroxysmal depolarizations, leading to repeated brisk firing correlated with the electroencephalogram (EEG) spikes, superimposed on a tonic hyperpolarization lasting for the entire SWD (Polack et al., 2007, 2009; Polack and Charpier, 2009; see also Figs. 1B and 2A3). Moreover, intracortical or systemic injection in the GAERS of ethosuximide, a first choice anti-absence drug, has an anti-epileptic effect (Manning et al., 2004; Polack and Charpier, 2009) that is correlated with the conversion of the hyperactive ictogenic cortical neurones into cortical neurones having normal electrophysiological properties (Polack and Charpier, 2009).

The cellular and network mechanisms controlling the paroxysmal discharges in the cortical ictogenic neurones remain unclear. Investigations in rodent genetic models of absence epilepsy, mostly conducted in slice preparations where seizure activity is absent, pointed out dysregulations in intrinsic and/or synaptic properties that could account for the propensity of somatosensory cortical neurones to gen-

[1] Present address: Department of Neurology, University of California Los Angeles, Los Angeles, CA 90095, USA.

*Correspondence to: S. Charpier, Centre de Recherche de l'Institut du Cerveau et de la Moelle épinière, UPMC/INSERM UMR-S 975, CNRS UMR 7225, Hôpital Pitié-Salpêtrière, 91 Boulevard de l'hôpital, F-75013, Paris, France. Tel: +33-1-40-77-99-16; fax: +33-1-40-77-99-13.

E-mail address: stephane.charpier@upmc.fr (S. Charpier).

*Abbreviations:* EEG, electroencephalogram; FS, fast-spiking; GAERS, Genetic Absence Epilepsy Rat from Strasbourg; IPSPs, inhibitory postsynaptic potentials; LTS, low-threshold spiking; SWD, spike-and-wave discharge.

0306-4522/11 $ - see front matter 
doi:10.1016/j.neuroscience.2011.06.037

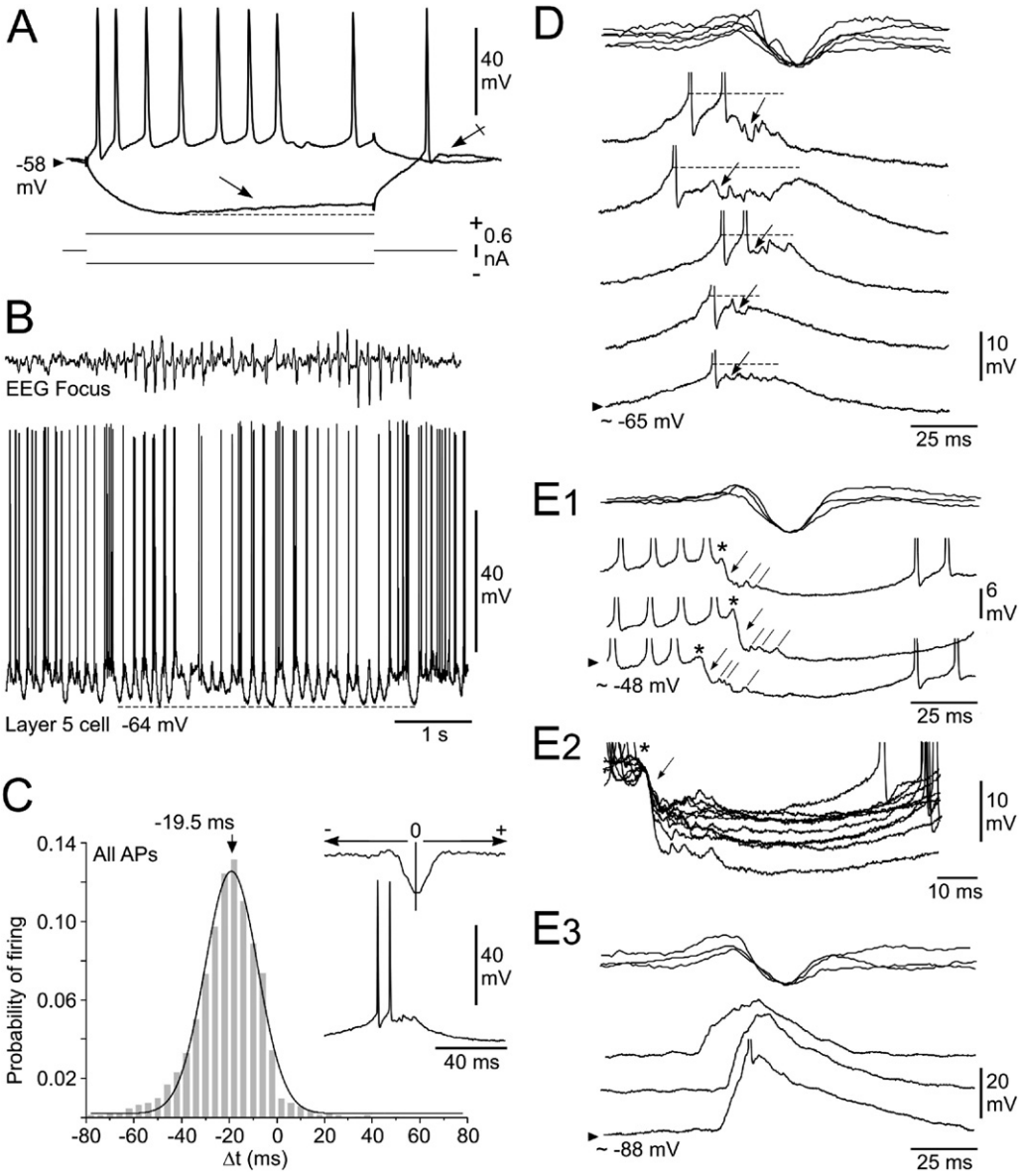


**Fig. 1.** Evidence for an inhibitory component during paroxysmal depolarizations in ictogenic neurones. (A) Intracellular responses (top records) to depolarizing and hyperpolarizing 200-ms current pulses (bottom traces) from a regular spiking neurone recorded in the layer 5 of the cortical focus. Note the sag in membrane voltage (arrow) during current-induced hyperpolarization and the rebound response at the break of the current pulse (crossed arrow). (B) Intracellular activity of the neurone shown in (A) (bottom traces) simultaneously recorded with the focus EEG (top traces). The occurrence of an SWD in the EEG was accompanied in the ictogenic neurone by rhythmic paroxysmal depolarizations, which were superimposed on a tonic membrane hyperpolarization (dashed line). (C) Pooled distribution of the timing (Δt) of all action potentials (APs; bin size, 4 ms) in ictogenic neurones ($n=12$), using the peak of the EEG spike as the zero-time reference (inset). The distribution was best fitted by a single Gauss-Laplace curve ($r^2=0.99$). Here and in the following figures, the mean value of action potentials timing is indicated at the top of the histogram. (D) Expanded dual records from the experiment shown in (B). The peak of the EEG spike was used to align the intracellular (bottom traces) and EEG records (superimposed top traces). The initial firing on the paroxysmal depolarizations was followed by near threshold (dashed lines) excitatory and inhibitory (arrows) synaptic events. (E) Voltage-dependency of paroxysmal depolarizations. (E1) Three successive intracellular records (bottom traces) from an ictogenic cell, obtained during DC injection of +1 nA, and the corresponding EEG spikes (superimposed top traces). Note the early depolarizing event (asterisks) followed by a brisk hyperpolarization (arrows) and subsequent bunches of small depolarizations (oblique lines). (E2) Superimposition ($n=10$) of the complex synaptic sequences during DC depolarization. The onset of the hyperpolarizing breaks (arrow), which disrupted the initial depolarization (asterisk), was used to align the records. (E3) Same representation as in (E1). The DC (−1 nA) hyperpolarization abolished the hyperpolarizing events and made emerge a large, up to 30 mV, depolarizing shift. In (D, E), action potentials are truncated for commodity. Here and in the following figures, the value of membrane potential is indicated by the arrowhead at the left of the intracellular record.

erate epileptic discharges. Specifically, the exacerbated activity of deep-layer neurones of the cortical focus could result from an increased expression of voltage-gated sodium channels (Klein et al., 2004) and/or a reduction in the dendritic hyperpolarization-activated inward cationic current ($I_h$) (Strauss et al., 2004). An increase in glutamatergic

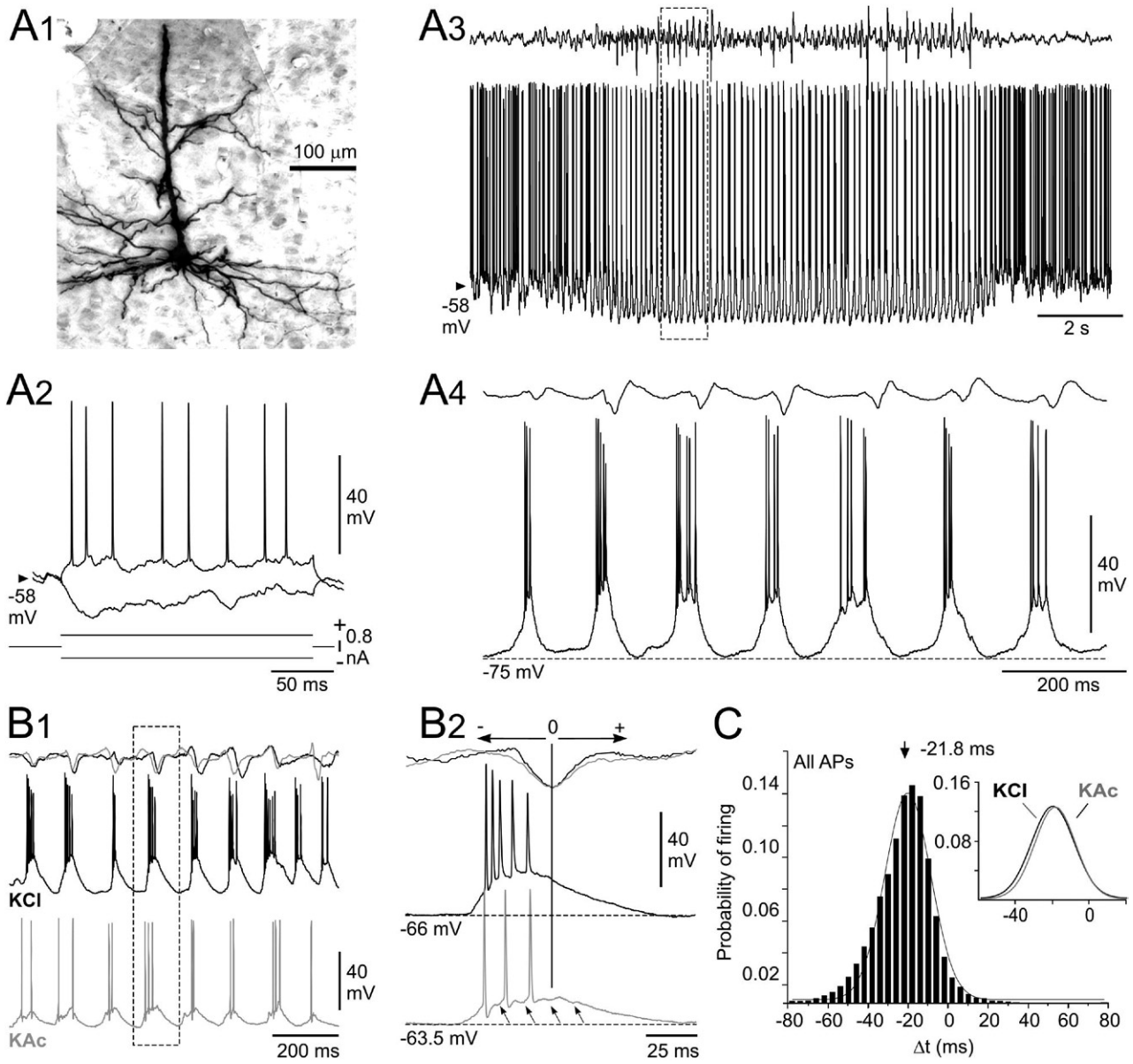


**Fig. 2.** Activity of cortical ictogenic neurones recorded with KCl-filled microelectrodes. (A) Morphological and electrophysiological properties of $Cl^-$-loaded ictogenic neurones. (A1) Microphotograph of a $Cl^-$-filled pyramidal neurone located in the layer 6 of the cortical focus. (A2) Voltage responses (top records) of the neurone shown in (A1) to depolarizing and hyperpolarizing current pulses (bottom traces). (A3) Spontaneous intracellular activity of the same neurone (bottom record) at the occurrence of an SWD in the related EEG (top record). (A4) Expansion of the paired recordings as indicated by the dashed box in (A3). The horizontal dashed line indicates the membrane potential reached during the seizure. (B) Increase of ictal firing rate after intracellular injection of $Cl^-$. (B1) Seizure activity in ictogenic neurones, recorded with KCl (black bottom trace) and KAc (grey bottom trace) electrodes in the same experiment, and corresponding paroxysmal EEGs (top traces). (B2) Expansion of the paired records as indicated by the dashed box in (B1). The amplitude of depolarizing shift and firing rate in the $Cl^-$-filled neurone (black trace) were both increased compared to those recorded with KAc electrode (grey trace). Note the small hyperpolarizing events in the KAc record (arrows), which disappeared when the cell was loaded with $Cl^-$. (C) Pooled distribution of the timing ($\Delta t$) of all action potentials (APs; bin size, 4 ms) in $Cl^-$-filled ictogenic neurones ($n=7$), using the peak of the EEG spike as the zero-time reference (B2). The distribution was best fitted by a Gauss-Laplace curve ($r^2=0.98$). The inset shows the superimposition of the fitting curves of firing distribution from pyramidal ictogenic neurones recorded with KAc (from Fig. 1C) and KCl electrodes.

NMDA-dependent conductance, together with a decrease in $GABA_A$ receptor-mediated synaptic transmission, has also been proposed as a potent mechanism for the paroxysmal depolarizing shifts in focus neurones (D'Antuono et al., 2006). This mechanism is supported by the reduction in the number and duration of SWDs after *in vivo* microinjection of $GABA_A$ positive allosteric modulators into the primary somatosensory cortex (Citraro et al., 2006). Moreover, the activation or blockade of group-II metabotropic glutamate receptors has a pro- or anti-epileptic effect, respectively, suggesting a role of these glutamate receptors in the pathogenesis of absence epilepsy (Ngomba et

al., 2005). Thus, converging data strongly suggest a crucial implication of the cortical glutamatergic and GABAergic synaptic systems in the generation of SWDs. However, the direct participation of a GABAergic component in the paroxysmal activity of the ictogenic neurones during absence seizures has never been explored.

Thus, the aim of the present study was to determine, by the means of *in vivo* paired EEG and intracellular recordings in the GAERS cortical focus, whether SWDs encompass an inhibitory synaptic component and to assess the role played by cortical inhibitory interneurones in the control of paroxysmal activities in ictogenic pyramidal cells.

## EXPERIMENTAL PROCEDURES

All animal experiments were performed in accordance with the European Communities Council Directive of 24 November 1986 (86/609/EEC) and every precaution was taken to minimize stress and the number of animals used in each series of experiments.

### Animal preparation

Experiments were performed *in vivo* on 17 adult (>15 weeks) GAERS. Animals were initially anesthetized with sodium pentobarbital (40 mg/kg, i.p.; Sanofi, Libourne, France) and ketamine (100 mg/kg, i.m.; Imalgène, Merial, France). A cannula was inserted into the trachea, and the animal was placed in a stereotaxic frame. Wounds and pressure points were repeatedly (every 2 h) infiltrated with lidocaïne (2%). Once the surgical procedures had been completed (see below), rats were analgesied and maintained in a narcotized and sedated state by injections of fentanyl (3 $\mu$g/kg, i.p.; Janssen-Cilag, Issy-les-Moulinaux, France) repeated every 20–30 min (Charpier et al., 1999; Polack and Charpier, 2009; Polack et al., 2007, 2009). To obtain long-lasting stable intracellular recordings, rats were immobilized with gallamine triethiodide (40 mg, i.m., every 2 h; Specia, Paris, France) and artificially ventilated. The degree of anesthesia was assessed by continuously monitoring the surface EEG and heart rate, and additional doses of fentanyl were administered at the slightest change toward an awaked pattern (i.e. an increase in the frequency and reduction in the amplitude of the EEG waves and/or an increase in heart beat rate). Body temperature was maintained (36.5–37.5 °C) with a homoeothermic blanket. At the end of the experiments, animals received an overdose of sodium pentobarbital (200 mg/kg, i.p.).

### Electrophysiological recordings

Surface EEG was made with a silver electrode (~60 k$\Omega$) placed on the dura above the facial region of the somatosensory cortex, which was demonstrated as the ictogenic region (focus) in GAERS (Polack and Charpier, 2009; Polack et al., 2007, 2009). Reference electrode was placed in a contralateral head muscle. Intracellular recordings were performed using glass micropipettes filled with 2 M KAc (50–80 M$\Omega$) or 3 M KCl (30–40 M$\Omega$). Pyramidal cells and interneurones were recorded within the layer 5-6 of the facial somatosensory cortex from the vicinity (<200 $\mu$m) of the EEG electrode, at the following coordinates: 7–9 mm anterior to the interaural line, 5–6 mm lateral to the midline, and 1.1–3.3 mm under the cortical surface (Polack and Charpier, 2009; Polack et al., 2007, 2009).

### Analysis

Intracellular recordings were obtained under current-clamp conditions using an Axoclamp-2B amplifier (Molecular Devices, Union City, CA, USA). Data were digitized for analysis at a sampling rate of 10 kHz for the intracellular signal and 1 kHz for EEG. Apparent membrane input resistance was measured from the mean ($n \geq 10$) membrane potential change in response to −0.4 or −0.6 nA current pulses (200 ms duration, repeated every 1.25 s) and the corresponding membrane time constant was the time taken for the membrane potential to reach 63% of its final value. Average membrane potential was determined during interictal periods from continuous recordings of at least 10 s. The voltage threshold of action potentials was measured as the membrane potential at which the $dV/dt$ exceeded 10 $V.s^{-1}$ (Polack et al., 2009). Their amplitude (50–70 mV) was calculated as the potential difference between the voltage threshold and the peak of the waveform, and their total duration was measured from the threshold to the return to this voltage reference.

Numerical values are given as means±SEM. Statistical significance was assessed with appropriate statistical tests, Student's unpaired *t*-test, Mann–Whitney rank sum-test or Levene median test. In some measurements, a Gauss-Laplace fit was performed. Statistical analyses and curve fitting were performed with Origin 7.5 (OriginLab Corporation, Northampton, MA, USA).

### Morphological identification

Some of recorded neurones were labelled using an intracellular injection of 1% neurobiotin tracer (Vector Laboratories, Burlingame, CA, USA) added to the pipette solution. Depolarizing current pulses (0.5–1 nA; 100–200 ms duration) were applied at a frequency of 1–2 Hz for a 15 min period. The histochemical methods used to reveal the morphology of neurobiotin-filled neurones are described in detail elsewhere (Polack and Charpier, 2006). The location of labelled neurones within the facial somatosensory cortex was determined using the atlas of Paxinos and Watson (1986).

## RESULTS

### SWD properties

The intra-SWD frequency was of 7.6±0.2 Hz ($n$=598 SWDs from 17 GAERS). SWDs had a duration of 14.9±2.4 s and recurred once every 19.9±3.8 s. These temporal properties of SWDs, as well as the shape of individual spike-wave complexes, are similar to those described previously under analogous experimental conditions (Charpier et al., 1999; Paz et al., 2007; Polack et al., 2007, 2009; Polack and Charpier, 2009) and in freely moving GAERS (Danober et al., 1998; Polack et al., 2007).

### The paroxysmal depolarizations in ictogenic neurones contain an inhibitory component

We first made *in vivo* intracellular recordings (using KAc electrodes) from the deep-layer pyramidal neurones ($n$=12 from eight GAERS) of the GAERS cortical focus, which were previously demonstrated as the neuronal trigger for cortico-thalamic SWDs (Paz et al., 2009; Polack and Charpier, 2009; Polack et al., 2007, 2009). Although the firing profile of focus pyramidal cells may vary in a state-dependent fashion, they displayed preferential current-evoked firing patterns, either regular spiking (Fig. 1A, $n$=6 neurones from five GAERS) or intrinsic bursting ($n$=6 neurones from three GAERS). Their mean input resistance and membrane time constant were 25.1±4.3 M$\Omega$ ($n$=11 neurones) and 7.4±1.0 ms ($n$=11 neurones), respectively (Fig. 1A). In most neurones ($n$=11), injection of large

amplitude hyperpolarizing current pulses disclosed a depolarizing sag (Fig. 1A arrow), likely due to $I_h$, followed by a post-anodal depolarization (Fig. 1A crossed arrow), possibly provoked by the slow kinetics of $I_h$ and/or by a low voltage-activated $Ca^{2+}$ current ($I_T$). Interictal activity of ictogenic cells was characterized by a noisy-like fluctuating membrane potential, averaging −58.2±0.7 mV ($n$=12 neurones) and generating a sustained discharge of action potentials (13.5±1.8 Hz; $n$=12 neurones) (Fig. 1B) having a mean voltage threshold of −52.3±0.7 mV ($n$=12 neurones).

The occurrence of an SWD was accompanied in focus neurones with rhythmic paroxysmal depolarizations, which had the same frequency as that of EEG spikes (7.5±0.2 Hz, $n$=12 neurones), superimposed on a tonic membrane hyperpolarization, which lasted for the entire seizure and reached an average value of −69.9±1.6 mV (from −77.2 to −61.6 mV, $n$=132 SWDs from 12 neurones) (Fig. 1B). The paroxysmal rhythmic depolarizations coincident with the EEG spikes were mostly (93%, $n$=8826 EEG spikes, $n$=12 neurones) suprathreshold, generating one to eight action potentials (1.8±0.3 action potentials). The corresponding mean firing rate during seizures was of 10.8±1.7 Hz (from 5 to 22.6 Hz, $n$=12 neurones) (Fig. 1B). The mean latency of the first action potential, relative to the peak negativity of the corresponding EEG spike (Fig. 1C, inset), was −24.4±1.5 ms (from −32 to −13 ms, $n$=8719 action potentials from 132 SWDs, $n$=12 neurones) (Fig. 4D1 inset, grey line). A similar analysis using all action potentials led to a unimodal distribution with a mean value of −19.5±1.4 ms ($n$=23,627 action potentials from 132 SWDs, $n$=12 neurones) (Fig. 1C). The patterns of neuronal activity, membrane properties and temporal relationships between cell discharge and EEG spikes, described above, are similar to those previously reported for ictogenic neurones initiating SWDs in the GAERS (Polack et al., 2007, 2009; Polack and Charpier, 2009).

A careful examination of the intracellular events concomitant with the EEG paroxysm (the “spike” component) revealed that the firing of ictogenic cells was interrupted by near threshold (∼−51 mV) upward and downward membrane potential fluctuations (Fig. 1D) resembling a mixture of excitatory and inhibitory synaptic events (Fig. 1D, arrows). To confirm the presence of an inhibitory component during EEG spikes, we made intracellular injection of DC depolarizing current (from 0.3 to 1 nA, $n$=5 neurones) to drive the membrane potential toward values (between −52 and −40 mV) expected to be less negative than the reversal potential of $GABA_A$ receptor-mediated inhibitory postsynaptic potentials (IPSPs) in somatosensory cortex pyramidal neurones, as calculated *in vivo* (∼−60 mV; Wilent and Contreras, 2004). This procedure unveiled a succession of synaptic events composed by an initial short depolarization (Fig. 1E1, E2, asterisks) abruptly interrupted by a hyperpolarization of 3–15 mV (Fig. 1E1, E2, arrows) having a fast kinetic (rise time <10 ms; Fig. 1E2, arrow) consistent with that previously described for $Cl^-$-dependent IPSPs in cortical neurones *in vivo* (Contreras et al., 1997; Timofeev et al., 2002). This fast hyperpolarization was followed by a cluster of small amplitude synaptic depolarizations (Fig. 1E1, oblique lines) and a slow repolarization lasting 40–50 ms. Consistent with intermingled excitatory and inhibitory synaptic events, a steady hyperpolarization (between −80 and −90 mV) of neurones by DC injection (−1 nA, $n$=5 neurones) resulted in a dramatic increase in the amplitude of the depolarizing shift (Fig. 1E3), likely caused by a reversion of GABAergic currents together with an augmentation in the driving force of glutamatergic events.

### Effects of intracellular injection of $Cl^-$ on the activity of ictogenic neurones

We demonstrated the existence of a $Cl^-$-dependent conductance in cortical focus pyramidal neurones (Fig. 2A1) during EEG paroxysms, and estimated its temporal properties, by making intracellular recordings ($n$=7 neurones from five GAERS) with KCl-filled microelectrodes. The mean interictal membrane potential of $Cl^-$-loaded neurones (−56.3±1.0 mV, $n$=7 neurones) was analogous to that calculated from neurones recorded with KAc electrodes ($P$=0.2). Their current-induced voltage responses were also similar (Fig. 2A2), with a roughly equal proportion of intrinsic bursting ($n$=3) and regular spiking ($n$=4) neurones (Fig. 2A2). However, $Cl^-$-filled neurones had a higher mean interictal firing rate (33.5±6.8 Hz, $n$=7 neurones; $P$<0.05) (Fig. 2A3), likely due to the occurrence of depolarizing $Cl^-$-dependent IPSPs, a process that is consistent with the sustained spontaneous discharge of inhibitory interneurones in between seizures (see Fig. 4A).

During SWDs, $Cl^-$-loaded neurones displayed rhythmic depolarizations (Fig. 2A3, A4), systematically suprathreshold and time-locked to the spike-and-wave complexes in the EEG (Fig. 2A4), superimposed on a tonic hyperpolarization reaching a mean value of −71.4±2.4 mV ($n$=109 SWDs from seven neurones) (Fig. 2A3, A4). The hyperpolarizing envelop was maintained throughout the seizure (Fig. 2A3), indicating that it was not due to a $Cl^-$-dependent conductance but rather to a synaptic disfacilitation, that is, a transient interruption in the tonic depolarizing synaptic drive (Charpier et al., 1999). As illustrated in the experiment shown in Fig. 2B, in which pyramidal neurones were recorded with KCl (black records) and KAc electrodes (grey records), the amplitude of paroxysmal depolarizing shifts was enhanced by $Cl^-$ infusion, provoking an increase in the number of action potentials per EEG spike (3.6±0.6 action potentials, from 4 to 11 action potentials, $n$=7 neurones; $P$=0.009) (Fig. 2B1, B2) that led to an augmentation in the mean ictal firing rate (25.7±4.6 Hz; $n$=7 neurones, $P$=0.04) (Fig. 2B1).

In $Cl^-$-loaded neurones, action potential discharge started −33.9±6.6 ms (from −54.6 to −18.3 ms, $n$=7 neurones) relative to the spike component of SWDs, a value similar to that measured with KAc electrode ($P$=0.2) (see aligned records in Fig. 2B2). Although the cell firing in association with the EEG spikes was increased after $Cl^-$ injection (see Fig. 2B1, B2), the mean latency of all action potentials (−21.8±3.2 ms, from −30.0 to −11.2 ms, $n$=32,777 action potentials from 109 SWDs, $n$=7 neu-

rones) (Fig. 2C) remained unchanged ($P=0.2$) (Fig. 2C inset). Moreover, we did not find any significant difference ($P>0.05$) between the temporal dispersions of action potential distributions in ictogenic cells recorded with KAc and KCl electrodes. Thus, the increase of firing rate in $Cl^-$-filled neurones was due to additional depolarization reflecting a postsynaptic $Cl^-$-dependent conductance, likely $GABA_A$-mediated and temporally confined to the depolarizing shift associated with the EEG spike.

### Rhythmic bursting in focus interneurones during absence seizures

We tested the hypothesis that the $Cl^-$-sensitive conductance in ictogenic neurones originated from intracortical GABAergic interneurones. We recorded from the two major classes of deep-layer GABAergic interneurones, the fast-spiking (FS) and low-threshold spiking (LTS) cells (Kawaguchi and Kubota, 1996, 1997), which produce a robust perisomatic and distal dendritic $GABA_A$ receptor-mediated inhibition of layer 5 pyramidal cells, respectively (Xiang et al., 2002; Markram et al., 2004). These cells ($n=7$ from six GAERS) were identified on the basis of electrophysiological criteria (Markram et al., 2004), including the characteristics of their action potential and their distinctive current-evoked firing patterns, which were in accordance with their non-pyramidal morphology, closely resembling that of layer 5 GABAergic basket cells (Fig. 3A1) (Kawaguchi and Kubota, 1997).

FS interneurones ($n=4$ from three GAERS) fired action potentials of $0.7\pm0.1$ ms duration, with pronounced and brief after-hyperpolarizations (Fig. 3A2, B). FS cells displayed current-evoked trains of action potentials, with little adaptation and instantaneous frequencies of up to 500 Hz, which could be transiently interrupted by a slowly depolarizing ramp (Fig. 3B), as previously observed (Kawaguchi and Kubota, 1996). LTS cells ($n=3$ from three GAERS) produced action potentials of longer duration ($1.1\pm0.1$ ms, Fig. 3A2) and fired repetitively, with a marked adaptation, when the depolarizing current pulse was applied from the rest ($\sim-58$ mV) (Fig. 3C). In LTS cells, a low-threshold depolarization (Fig. 3C, arrow), which could provoke typical burst-like discharge (Fig. 3C, inset), was generated at the break of hyperpolarizing pulses (Fig. 3C) or in response to depolarizing pulses only when applied from a hyperpolarized membrane potential (below $-65$ mV, not shown). FS and LTS interneurones had an apparent input resistance of $25.8\pm5.8$ ($n=4$ neurones) and $21.1\pm5.5$ MΩ ($n=3$ neurones), respectively.

Both types of interneurones exhibited during interictal periods background membrane potential fluctuations, averaging $-61.0\pm1.4$ mV ($n=7$ neurones), which provoked a spontaneous firing of $11.1\pm4.4$ Hz (Fig. 4A). As observed in pyramidal cells (see Fig. 1B), SWDs were concomitant in interneurones with rhythmic suprathreshold depolarizations, time-locked with the EEG spikes, superimposed on a membrane hyperpolarization ($-69.2\pm3.2$ mV, $n=7$ neurones) that persisted throughout the seizure (Fig. 4A). The paroxysmal depolarizations in FS neurones were progressively sculpted by the temporal summation of small synaptic events (Fig. 4B1, oblique lines and C, middle records), generating 2–11 action potentials with an instantaneous frequency ranging from 200 to 400 Hz (Fig. 4B1, C, middle records). In LTS cells, the paroxysmal shifts were composed of temporally summating high-frequency depolarizing synaptic potentials (Fig. 4B2, oblique lines) and a subsequent low-threshold spike giving rise to bursts of two to eight action potentials (Fig. 4B2).

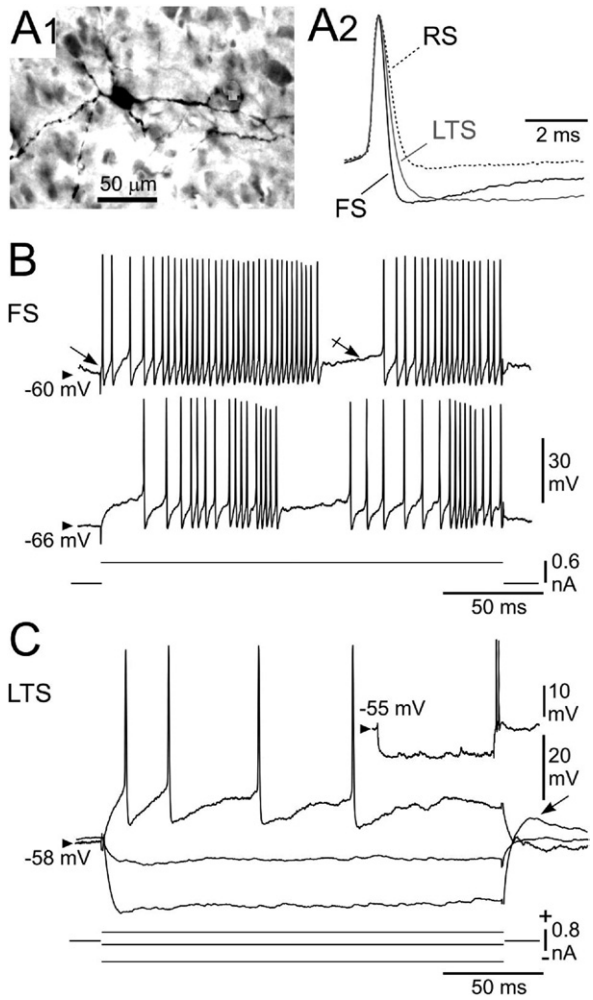


**Fig. 3.** Morpho-functional identification of GABAergic interneurones. (A1) Microphotograph of the somatodendritic region of a Neurobiotin-filled layer 5 neurone that displayed the morphological features of GABAergic basket cells (see Kawaguchi and Kubota, 1996). (A2) Superimposition of single action potentials recorded from RS, LTS and FS neurones. Amplitude of action potentials was normalized to highlight their different durations and distinct after-hyperpolarizations. (B) The FS cell showed an abrupt (arrow) discharge of high-frequency train of action potentials (top record), which could be momentary suspended by a slow depolarizing ramp (crossed arrow), in response to suprathreshold current pulses (bottom trace). (C) Voltage responses of an LTS cell to negative and positive current pulses. The LTS cell showed a firing pattern with a marked adaptation when activated from rest ($-58$ mV). Note the post-anodal depolarization (arrow) at the break of the largest hyperpolarizing current, which could generate a burst of action potentials (inset, 200 ms-current pulse of $-1$ nA).

In the experiments ($n=2$) in which regular spiking (pyramidal) and FS neurones were recorded in the same

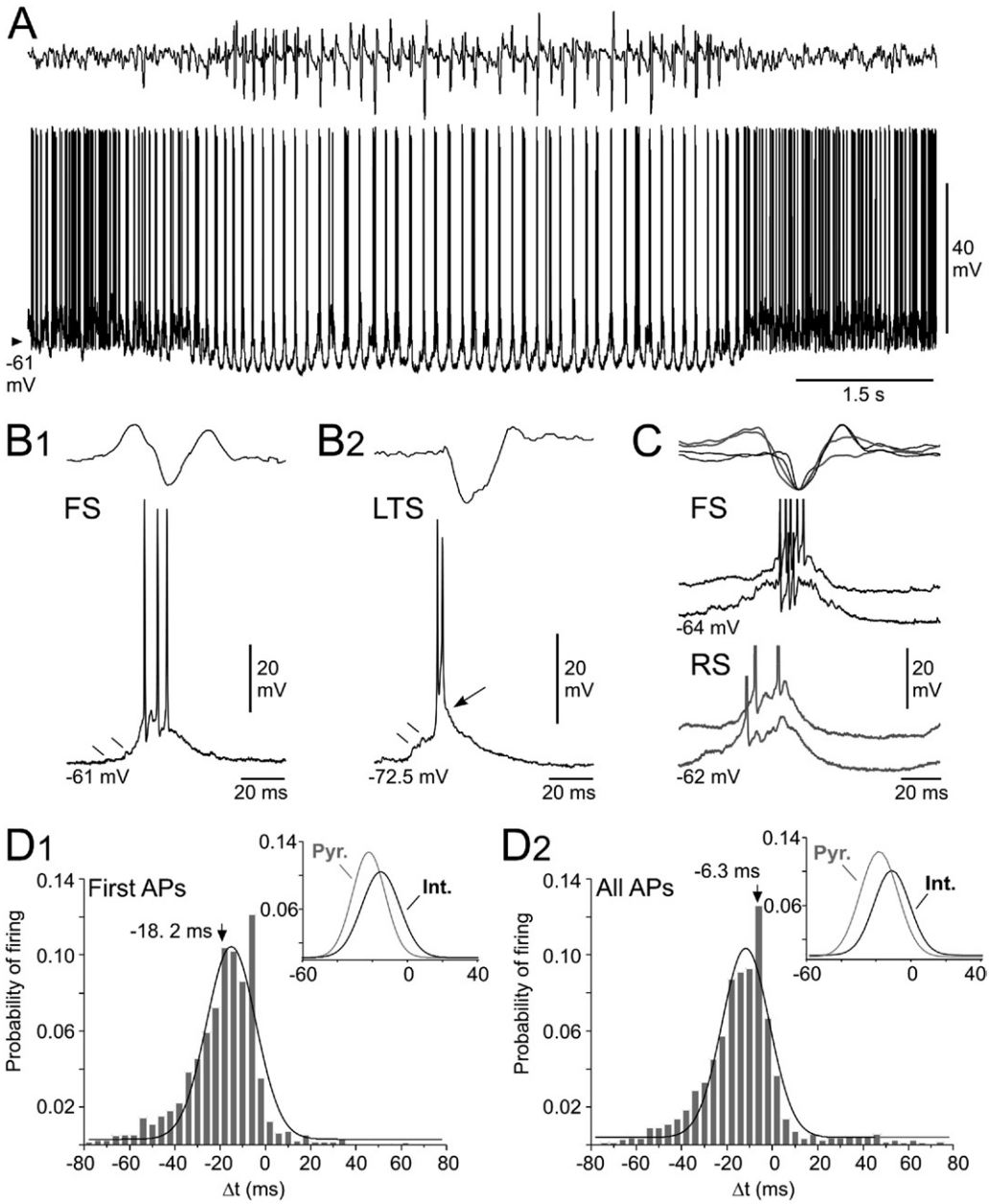


**Fig. 4.** Activity of cortical focus interneurones during SWDs. (A) Simultaneous recordings of the intracellular activity of an FS interneurone (same cell as in Fig. 3B) (bottom trace) and of the corresponding EEG (top trace). (B) Examples of paroxysmal depolarizations (bottom traces), coincident with the EEG spike (top records), recorded in FS (B1) and LTS (B2) neurones. In both cell types, the initial depolarization was sculpted by the temporal summation of brief depolarizing synaptic events (oblique lines), which were followed in the LTS cell by a low-threshold spike-like depolarization (arrow) crowned by a burst of action potentials. (C) EEG spikes (top records) and corresponding intracellular paroxysmal events ($n=2$) recorded in an FS cell (black traces) and in an RS neurone (grey traces) during the same experiment. Action potentials are truncated. (D) Temporal firing properties of interneurones in relation with EEG paroxysms. (D1) Pooled histogram (bin=4 ms) and Gauss-Laplace fit ($r^2=0.90$) showing the timing ($\Delta t$) of first action potentials (APs) ($n=7$ interneurones) relative to the peak negativity of the EEG spike (taken as time 0, see Fig. 1C). (D2) Same analysis as in (D1) using all action potentials during seizures ($n=7$ interneurones, bin=4 ms; $r^2$ of Gauss-Laplace fit=0.93). The mean values of the distributions are indicated. The insets in (D1, D2) show the superimpositions of Gauss-Laplace fits computed from ictogenic pyramidal cells (Pyr., grey lines) and focus interneurones (Int., black lines).

GAERS (Fig. 4C), the paroxysmal firing of the presumed GABAergic interneurones shortly followed that of the pyramidal cells and coincided with the late mixed synaptic potentials, which contain the inhibitory $Cl^-$-mediated synaptic component (see Figs. 1D and 2B2). The relatively delayed discharge of inhibitory interneurones during seizures was statistically confirmed by the latency of their first action potential, using the EEG spike as the temporal reference (as indicated in Fig. 1C), which averaged $-18.2\pm3.3$ ms ($n=3939$ action potentials from 289 SWDs, $n=7$ neurones) (Fig. 4D1), corresponding to a time-lag of $+7.9$ ms compared to the pyramidal cells (Fig. 4D1, inset).

Using all action potentials, the pooled distribution of firing probability in cortical interneurones was unimodally distributed with a mean value of $-6.3\pm6.0$ ms (8693 action potentials, from 289 SWDs, $n=7$ neurones) (Fig. 4D2), corresponding to a significant ($P=0.003$) temporal delay of $+13.3$ ms compared to paroxysmal discharges in pyramidal ictogenic neurones (see Fig. 4D2, inset). Altogether, these findings indicate that the ictal firing of cortical interneurones shortly follows that of pyramidal ictogenic neurones and coincides with the $Cl^-$-mediated synaptic events.

## DISCUSSION

The purpose of the present study was to explore the possible participation of the intracortical inhibitory system in the paroxysmal activity of cortical neurones initiating genetically-determined absence seizures. First, we found that DC depolarization of the ictogenic cells during seizures unmasked brief synaptic depolarizations disrupted by hyperpolarizing events, which may reflect $GABA_A$ receptor-mediated IPSPs. This was subsequently confirmed by intracellular injection of $Cl^-$ that dramatically increased the amplitude of the rhythmic depolarizations and the number of generated action potentials. The $Cl^-$-dependent conductance, overlapping the paroxysmal depolarization of ictogenic cells and limiting their firing rate, was correlated with the discharge of intracellularly recorded cortical interneurones. These findings suggest that epileptic discharges in ictogenic pyramidal cells are negatively controlled by a fast feedback $Cl^-$-dependent inhibition resulting from the recurrent activation of GABAergic interneurones.

### GABAergic control of SWDs

The present study provides the first evidence for an inhibitory synaptic component in the cortical paroxysms during spontaneous, genetically-determined, SWDs. In a previous *in vivo* investigation from a pharmacological cat model of cortically-generated spike-and-wave activity, mimicking the Lennox–Gastaut seizures, it has been shown that the repeated firing of cortical GABAergic interneurones during seizures produced a prolonged opening of $Cl^-$ channels in neighbouring pyramidal neurones, which resulted in an increase in the intracellular concentration of $Cl^-$ and a positive shift in its reversal potential (Timofeev et al., 2002). In such a condition, the IPSPs become depolarizing and facilitate the development of seizures.

Here, we found that a $Cl^-$-dependent synaptic component coincides with the paroxysmal shift in ictogenic neurones but becomes inhibitory when the membrane potential approaches action potential threshold. Although the exact value of $Cl^-$ reversal potential was not measured in our study, hyperpolarizing synaptic events could not be detected at potentials lower than $\sim-62$ mV but were clearly identified at potentials just below or slightly above action potential threshold ($\sim-51$ mV) (see Figs. 1D, E1, E2 and 4C), strongly suggesting a reversal potential close to that calculated *in vivo* from non-epileptic somatosensory cortex pyramidal neurones ($\sim-60$ mV; Wilent and Contreras, 2004).

According to the findings obtained in the present study, we can propose the following sequence of intracellular excitatory and inhibitory events in ictogenic neurones during SWDs. During a spike-and-wave complex, the initial component of the paroxysmal depolarizing shift is likely due to excitatory synaptic interactions between glutamatergic deep-layer pyramidal neurones of the focus, since this cell population fires before the other sources of excitatory inputs, such as pyramidal neurones located in the upper layers of the focus, pyramidal cells in distant cortical areas and thalamo-cortical afferents (Polack et al., 2007, 2009). We cannot exclude the subsequent participation of excitatory thalamic inputs, although the discharge of thalamo-cortical cells during absence seizures has been found relatively moderate (Paz et al., 2009; Polack et al., 2009). It is also plausible that the synaptic depolarization of focus pyramidal neurones be amplified by an increase in persistent voltage-gated $Na^+$ current (González-Burgos and Barrionuevo, 2001; Klein et al., 2004), which could also account for their elevated tonic firing and bursting activity (Aracri et al., 2006; Hutcheon et al., 1996). The membrane depolarization could be further facilitated by the fast activation, from the hyperpolarizing envelop, of $I_h$, which has been disclosed in the ictogenic cells during injection of negative current (Polack et al., 2009; see also Fig. 1A). Altogether, these synaptic and intrinsic processes could underlie the paroxysmal depolarization and the discharge of action potentials in ictogenic neurones during SWDs. The synaptically-induced firing of interneurones that rapidly follows ($\sim+8$ ms) the discharge of ictogenic neurones (see Fig. 4D1) strongly suggests a fast recurrent activation of interneurones by focus pyramidal neurones (Silberberg, 2008). In turn, the repeated bursting of interneurones during cortical paroxysms, while the membrane depolarization of postsynaptic pyramidal neurones exceeds the reversal potential of $Cl^-$, will produce a hyperpolarizing synaptic inhibition interfering with the synaptic excitation and limiting the firing of ictogenic cells. Such a negative GABAergic control of ictogenic neurones during paroxysmal depolarizing shifts is corroborated by the fast hyperpolarizing events that interrupt cell discharge (see Fig. 1D), the large-amplitude synaptic hyperpolarization unmasked by DC depolarization (see Fig. 1E1, E2), the firing of interneurones that largely coincides with the IPSPs and the strong $Cl^-$-dependent conductance in ictogenic cells (see Figs. 2B, C vs. 4D).

Somatosensory cortical neurones from non-epileptic rats, as well as GAERS cortical pyramidal neurones recorded outside the cortical focus, are more hyperpolarized and less active, during and in between SWDs, compared to GAERS pyramidal focus neurones (Polack et al., 2007, 2009; Polack and Charpier, 2009). It is thus plausible that the GABAergic inhibitory transmission within the focus, although efficient to limit the firing rate of ictogenic cells as demonstrated in this study, is partially altered (D'Antuono et al., 2006) compared to other cortical regions. Moreover, it is possible that the recruitment of rhythmic inhibitory

interneurones partly participates to the progressive slowing of the internal frequency of focus SWDs, from 10 to 12 Hz at the onset of paroxysm to a relatively stable 7 Hz oscillation during the main body of the seizure (Polack et al., 2007). Indeed, the relatively high amplitude and long duration of inhibitory synaptic conductance, compared to excitatory events (Haider et al., 2006), can rapidly decrease the frequency of cortical oscillations on a cycle-to-cycle basis (Atallah and Scanziani, 2009).

### Functional consequences

The present findings demonstrate an active $Cl^-$-mediated synaptic inhibition of cortical cells during SWDs. This contrasts with other forms of ictal activities, such as temporal lobe seizures, in which a depolarizing shift in the $Cl^-$ reversal potential in ictogenic neurones is responsible for a depolarizing and pro-epileptic effect of $GABA_A$ synaptic inputs (Khalilov et al., 2003; Huberfeld et al., 2007). The opposite effect of the GABAergic system in these two forms of epilepsy could also account, at least in part, for the relative exacerbated depolarization and firing rate in epileptogenic pyramidal hippocampal neurones *in vivo* as compared to GAERS cortical focus neurones (Fig. 2C in Langlois et al., 2010 vs. Fig. 1B).

During absence seizures, the rhythmic spiking activity of cortical GABAergic interneurones evokes a substantial postsynaptic inhibition allowing ictogenic neurones to restrict their discharge within a relatively tight temporal window at the initial phase of the paroxysmal depolarization. This could effectively phase firing and oscillatory behaviour in the ictogenic pyramidal cells (Cobb et al., 1995) at the frequency of SWDs. Moreover, this GABAergic mechanism could also promote the firing coherence among ictogenic pyramidal cells, by constraining the discharge of the pyramidal neurones population within a fixed time window, and thus facilitate the propagation and the generalization of epileptic activities in the cortico-thalamic networks (Paz et al., 2009; Polack et al., 2009).

The presynaptic inhibitory interneurones could also provide a potent intracortical system for seizure cessation. The transition from bursting to tonic discharge in thalamo-cortical neurones in the GAERS (Paz et al., 2007), which spontaneously occurs just before the end of the seizure (Paz et al., 2009), results in an interruption of SWDs that is correlated in layer 5 cortical neurones with a membrane hyperpolarization, a diminution in their firing rate and a reduction in their membrane input resistance. It is plausible that the increased tonic activity of thalamo-cortical cells, around the termination of seizures, causes a widespread feed-forward cortical inhibition by the massive recruitment of cortical GABAergic interneurones (Swadlow, 2003). This would thus result in an increase in the membrane conductance of cortical ictogenic neurones and a powerful shunting inhibition of their excitatory synaptic inputs (Staley and Mody, 1992), repressing their endogenous propensity to maintain ictal activities.

*Acknowledgments—This work was supported by grants from the Agence Nationale de la Recherche (ANR RO6275CS, 2006), the Fédération pour la Recherche sur le Cerveau (FRC-2010), the Institut National de la Santé et de la Recherche Médicale, the Centre National de la Recherche Scientifique and l'Université Pierre et Marie Curie (Paris 6). Mathilde Chipaux was supported by a Ligue Française Contre l'Epilepsie (LFCE) doctoral fellowship. We thank Dr. S. Mahon for thoughtful comments and critical reading of the manuscript.*

## REFERENCES

Aracri P, Colombo E, Mantegazza M, Scalmani P, Curia G, Avanzini G, Franceschetti S (2006) Layer-specific properties of the persistent sodium current in sensorimotor cortex. J Neurophysiol 95:3460–3468.

Atallah BV, Scanziani M (2009) Instantaneous modulation of gamma oscillation frequency by balancing excitation with inhibition. Neuron 62:566–577.

Bal T, von Krosigk M, McCormick DA (1995) Role of the ferret perigeniculate nucleus in the generation of synchronized oscillations *in vitro*. J Physiol 483:665–685.

Buzsáki G (1991) The thalamic clock: emergent network properties. Neuroscience 41:351–364.

Charpier S, Leresche N, Deniau JM, Mahon S, Hughes SW, Crunelli V (1999) On the putative contribution of GABA(B) receptors to the electrical events occurring during spontaneous spike and wave discharges. Neuropharmacology 38:1699–1706.

Citraro R, Russo E, Di Paola ED, Ibbadu GF, Gratteri S, Marra R, De Sarro G (2006) Effects of some neurosteroids injected into some brain areas of WAG/Rij rats, an animal model of generalized absence epilepsy. Neuropharmacology 50:1059–1071.

Cobb SR, Buhl EH, Halasy K, Paulsen O, Somogyi P (1995) Synchronization of neuronal activity in hippocampus by individual GABAergic interneurons. Nature 378:75–78.

Contreras D, Destexhe A, Steriade M (1997) Intracellular and computational characterization of the intracortical inhibitory control of synchronized thalamic inputs *in vivo*. J Neurophysiol 78:335–350.

D'Antuono M, Inaba Y, Biagini G, D'Arcangelo G, Tancredi V, Avoli M (2006) Synaptic hyperexcitability of deep layer neocortical cells in a genetic model of absence seizures. Genes Brain Behav 5:73–84.

Danober L, Deransart C, Depaulis A, Vergnes M, Marescaux C (1998) Pathophysiological mechanisms of genetic absence epilepsy in the rat. Prog Neurobiol 55:27–57.

González-Burgos G, Barrionuevo G (2001) Voltage-gated sodium channels shape subthreshold EPSPs in layer 5 pyramidal neurons from rat prefrontal cortex. J Neurophysiol 86:1671–1184.

Haider B, Duque A, Hasenstaub AR, McCormick DA (2006) Neocortical network activity *in vivo* is generated through a dynamic balance of excitation and inhibition. J Neurosci 26:4535–4545.

Holmes MD, Brown M, Tucker DM (2004) Are "generalized" seizures truly generalized? Evidence of localized mesial frontal and frontopolar discharges in absence. Epilepsia 45:1568–1579.

Huberfeld G, Wittner L, Clemenceau S, Baulac M, Kaila K, Miles R, Rivera C (2007) Perturbed chloride homeostasis and GABAergic signaling in human temporal lobe epilepsy. J Neurosci 27: 9866–9873.

Hutcheon B, Miura RM, Puil E (1996) Subthreshold membrane resonance in neocortical neurons. J Neurophysiol 76:683–697.

Kawaguchi Y, Kubota Y (1996) Physiological and morphological identification of somatostatin- or vasoactive intestinal polypeptide-containing cells among GABAergic cell subtypes in rat frontal cortex. J Neurosci 16:2701–2715.

Kawaguchi Y, Kubota Y (1997) GABAergic cell subtypes and their synaptic connections in rat frontal cortex. Cereb Cortex 7: 476–486.

Khalilov I, Holmes GL, Ben-Ari Y (2003) *In vitro* formation of a secondary epileptogenic mirror focus by interhippocampal propagation of seizures. Nat Neurosci 6:1079–1085.

Klein JP, Khera DS, Nersesyan H, Kimchi EY, Waxman SG, Blumenfeld H (2004) Dysregulation of sodium channel expression in cortical neurons in a rodent model of absence epilepsy. Brain Res 1000:102–109.

Langlois M, Polack PO, Bernard H, David O, Charpier S, Depaulis A, Deransart C (2010) Involvement of the thalamic parafascicular nucleus in mesial temporal lobe epilepsy. J Neurosci 30:16523–16535.

Manning JP, Richards DA, Leresche N, Crunelli V, Bowery NG (2004) Cortical-area specific block of genetically determined absence seizures by ethosuximide. Neuroscience 123:5–9.

Markram H, Toledo-Rodriguez M, Wang Y, Gupta A, Silberberg G, Wu C (2004) Interneurons of the neocortical inhibitory system. Nat Rev Neurosci 5:793–807.

Meeren HK, Pijn JP, van Luijtelaar EL, Coenen AM, Lopes da Silva FH (2002) Cortical focus drives widespread corticothalamic networks during spontaneous absence seizures in rats. J Neurosci 22:1480–1495.

Ngomba RT, Biagioni F, Casciato S, Willems-van Bree E, Battaglia G, Bruno V, Nicoletti F, van Luijtelaar EL (2005) The preferential mGlu2/3 receptor antagonist, LY341495, reduces the frequency of spike-wave discharges in the WAG/Rij rat model of absence epilepsy. Neuropharmacology 49 (Suppl 1):89–103.

Panayiotopoulos CP (1997) Absence epilepsies. In: Epilepsy: a comprehensive textbook (Engel J, Pedley TA, eds), pp 2327–2346. Philadelphia: Lippincot-Raven.

Paxinos G, Watson C (1986) The brain in stereotaxic coordinates. Sydney: Academic.

Paz JT, Chavez M, Saillet S, Deniau JM, Charpier S (2007) Activity of ventral medial thalamic neurons during absence seizures and modulation of cortical paroxysms by the nigrothalamic pathway. J Neurosci 27:929–941.

Paz JT, Polack PO, Slaght SJ, Deniau JM, Chavez M, Mahon S, Charpier S (2009) Cortical initiation of absence seizures, propagation to basal ganglia and back to the cortex. In: Pan-brain abnormal neural network in epilepsy (Tang FR, ed), pp 41–65. India, Kerala: Research Signpost.

Polack PO, Charpier S (2006) Intracellular activity of cortical and thalamic neurones during high-voltage rhythmic spike discharge in Long-Evans rats *in vivo*. J Physiol 571:461–476.

Polack PO, Charpier S (2009) Ethosuximide converts ictogenic neurons initiating absence seizures into normal neurons in a genetic model. Epilepsia 50:1816–1820.

Polack PO, Guillemain I, Hu E, Deransart C, Depaulis A, Charpier S (2007) Deep layer somatosensory cortical neurons initiate spike-and-wave discharges in a genetic model of absence seizures. J Neurosci 27:6590–6599.

Polack PO, Mahon S, Chavez M, Charpier S (2009) Inactivation of the somatosensory cortex prevents paroxysmal oscillations in cortical and related thalamic neurons in a genetic model of absence epilepsy. Cereb Cortex 19:2078–2091.

Sadleir LG, Farrell K, Smith S, Connolly MB, Scheffer IE (2006) Electroclinical features of absence seizures in childhood absence epilepsy. Neurology 67:413–418.

Silberberg G (2008) Polysynaptic subcircuits in the neocortex: spatial and temporal diversity. Curr Opin Neurobiol 18:332–337.

Staley KJ, Mody I (1992) Shunting of excitatory input to dentate gyrus granule cells by a depolarizing GABAA receptor-mediated postsynaptic conductance. J Neurophysiol 68:197–212.

Strauss U, Kole MH, Bräuer AU, Pahnke J, Bajorat R, Rolfs A, Nitsch R, Deisz RA (2004) An impaired neocortical Ih is associated with enhanced excitability and absence epilepsy. Eur J Neurosci 19:3048–3058.

Swadlow HA (2003) Fast-spike interneurons and feedforward inhibition in awake sensory neocortex. Cereb Cortex 13:25–32.

Timofeev I, Grenier F, Steriade M (2002) The role of chloride-dependent inhibition and the activity of fast-spiking neurons during cortical spike-wave electrographic seizures. Neuroscience 114:1115–1132.

Westmijse I, Ossenblok P, Gunning B, van Luijtelaar G (2009) Onset and propagation of spike and slow wave discharges in human absence epilepsy: A MEG study. Epilepsia 50:2538–2548.

Wilent WB, Contreras D (2004) Synaptic responses to whisker deflections in rat barrel cortex as a function of cortical layer and stimulus intensity. J Neurosci 24:3985–3998.

Williams D (1953) A study of thalamic and cortical rhythms in petit mal. Brain 76:56–69.

Xiang Z, Huguenard JR, Prince DA (2002) Synaptic inhibition of pyramidal cells evoked by different interneuronal subtypes in layer V of rat visual cortex. J Neurophysiol 88:740–750.

*(Accepted 11 June 2011)*
*(Available online 24 June 2011)*